



OPEN

# Altering ROY polymorph crystallization in conventional and microfluidic crystallizers with acoustic cavitation

Mohammed Noorul Hussain✉, Arthur Demuyck &amp; Tom Van Gerven

Selective crystallization of polymorphs can be a difficult task, influenced by several physical and chemical parameters like mixing, temperature, supersaturation, solvent, etc. Acoustic cavitation, produced at low ultrasonic frequencies, induces effects like micro-mixing and local heating which, when coupled to crystallization, can alter crystal form nucleation. In this work, anti-solvent crystallization of a model compound (ROY) was conducted to investigate the effect of acoustic cavitation on polymorph nucleation. Experiments were conducted in batch and microfluidic flow crystallization setups at different anti-solvent volume fractions under silent and sonicated conditions. Results show that sonication has a significant effect on the polymorphic outcome. In batch crystallization sonication promoted the formation of the stable Y form. This observation was consistent for flow crystallization experiments at a low flow rate. At a higher flow rate, this effect weakened due to low residence times. In some batch experiments recorded with a high speed camera it was found that the formation of the Y form was most probably facilitated by ultrasound enhanced polymorphic transformation rather than direct nucleation. Additionally, computational fluid dynamic simulations (only silent-flow conditions) indicate that supersaturation distribution within the channel has a significant effect on the polymorph nucleated.

**Keywords** Polymorphs, Microfluidics, Crystallization, Acoustic cavitation

Polymorphism is the ability of a compound to exist in several crystal forms without a change in its chemical composition. Different polymorphs can have different density, solubility, melting point etc<sup>1</sup>. Such differences can significantly affect the usage of the crystalline compound in its intended application. Controlling crystallization outcome in systems where the compound can crystallize in different polymorphs can be a challenging task. Crystallization of the right polymorph involves controlling multiple chemical and physical parameters. Chemical parameters can include choice of solvent and anti-solvent, concentration/supersaturation, pH etc. Physical parameters can include temperature, pressure, mixing etc.

Mixing plays an important role in crystallization and especially anti-solvent crystallization. Uniform mixing of solvent and anti-solvent in the system is quite important as any imbalances can have an effect on which polymorph nucleates<sup>2</sup>. Ultrasound is an excellent mixing technique which is proven to enhance crystallization processes in many ways<sup>3-5</sup>. It can be applied in both batch and flow systems. Ultrasound is not just a mixing technique but it also exhibits different physical sub-phenomena depending on the applied frequency. At low frequencies ultrasound exhibits acoustic cavitation while at higher frequencies acoustic streaming is predominant<sup>6,7</sup>. Acoustic cavitation is a phenomenon where a large number of micron sized bubbles are produced during the low pressure cycle of the acoustic wave. These bubbles have extremely high temperature and pressure within them, in the range of 1000's of K and 1000's of Pa<sup>8</sup>. These bubbles undergo compression and expansion following the cycles of the acoustic wave. Some bubbles collapse violently under the influence of high acoustic pressures. It is a powerful phenomenon which in some cases has also shown an effect on polymorph selectivity<sup>9</sup>. In addition, the collapse of the bubbles produces micro shock waves and turbulence, which can significantly enhance local mixing and thereby improve both local and bulk mixing.

Continuous flow crystallization is gaining prominence as a method of crystallization due to its numerous advantages over batch crystallization<sup>10</sup>. Some of the main benefits are the enablement of homogeneous conditions due to miniaturized volumes, eliminating the problem of batch to batch variation, better conservation of materials

ProcESS Division, Department of Chemical Engineering, KU Leuven, Leuven, Belgium. ✉email: mohammednoorul.hussain@uantwerpen.be

in case of malfunction, better process safety etc<sup>10</sup>. Despite such benefits the fully fledged application of flow crystallization in the industry is still facing some hurdles. One such hurdle is the lack of sufficient understanding and investigation of flow crystallization with polymorph selectivity. It is very important to understand the polymorph nucleation behavior of different compounds in a flow system since the behavior of crystallization can be very different in comparison to batch systems.

5-methyl-2-[(2-nitrophenyl)amino]-3-thiophenecarbonitrile, better known as ROY (called after the colors of its polymorphs: “Red, Orange, Yellow”), was initially synthesized as a precursor for olanzapine which is an anti-psychotic drug<sup>11</sup>. The polymorphism of ROY is very interesting as it has a high number of polymorphs which also exhibit varying colors like red, orange and yellow. The crystals that can be formed from a solution are: Red prisms (R), Yellow prisms (Y), Orange Needles (ON), Orange Plates (OP), Yellow Needles (YN), Orange Red Plates (ORP) and deep Red blocks (R18)<sup>12</sup>. For anti-solvent crystallization, with acetone as the solvent and water as the anti-solvent, at 20 °C and atmospheric pressure it was found that in equilibrium conditions at low volume fraction (VF) of anti-solvent R and Y dominate. In intermediate VF, OP and ON are present. At high VF, ON and YN are the most common<sup>13</sup>. Mixing and temperature play an important role in ROY polymorph nucleation as was found by Nerom et. al<sup>13</sup> and Ziemecka et al.<sup>11</sup>. Improper mixing can lead to nucleation of metastable polymorphs.

In this work, both batch and flow anti-solvent crystallization experiments of ROY were performed under silent and sonicated conditions. A lower acoustic frequency was consistently chosen to ensure an acoustic cavitation regime. To the best of the authors’ knowledge there are no studies investigating the effect of acoustic cavitation where factors like cavitation bubble implosion aided local temperature and pressure variations can play a role. Experiments were conducted at different anti-solvent volume fractions (VFs) and different flow rates (for flow experiments). Product crystals were analyzed not just by light microscopy but also with ATR-FTIR (Attenuated Total Reflectance Fourier Transform Infrared Spectroscopy). Some experiments were also conducted to study the extent of polymorph transformation during the process. A Computational Fluid Dynamics (CFD) study was conducted to simulate the distribution of solution and anti-solvent in the flow crystallizer channel under silent conditions to correlate with flow crystallization experiments. The main aim of this work was to investigate the polymorphs formed in the chosen conditions and to understand the mechanism behind it. The broader objective was to gain insight into the impact of conditions created by acoustic cavitation on the crystallization process of a polymorphic compound.

## Methodology

5-Methyl-2-((2-nitrophenyl)amino)-3-thiophenecarbonitrile (99%) i.e., ROY (Red Orange Yellow) was obtained from Toronto Research Chemicals Inc. and was analyzed as red prisms using microscope and ATR-FTIR (Perkin-Elmer Spectrum 100 with UATR accessory). Acetone (HPLC grade Fischer Scientific) was used as solvent and DI water was used as anti-solvent in all cases. Since there was no solubility data available in literature for ROY at different acetone-water mixtures, solubility at the tested VFs was estimated using High-Performance Liquid Chromatography. More information on the procedure is provided in the supplementary information. The solubility measured at 0.2 VF (at 20 °C) was estimated to be 19.7 mg/mL. The solubility already drops significantly to 4.3 mg/mL at 0.4 VF. For a VF of 0.85 the solubility dropped to near zero values.

Batch experiments were conducted in a temperature controlled, jacketed crystallizer with a volume of 3 mL. First, 0.5 mL of the ROY-acetone solution was added into the crystallizer. An overhead mixer was then placed inside the crystallizer and was set to 300 rpm. The anti-solvent was then added at different volumes in separate experiments to reach VFs of 0.2, 0.4 and 0.85. The temperature was controlled at 20 °C by a thermal bath (Julabo 600 F) running water in the jacket. Calorimetric measurements were performed by measuring the temperature using a Picolog data recorder and a thermocouple. A graphical representation of the setup can be seen in Fig. 1a. The slurry after crystallization was filtered in a vacuum filtration setup using a 0.22 µm pore size filter. For sonicated batch experiments, the crystallizer was mounted on a transducer (USworld - MPI-7850D-20\_40\_60H) connected to an amplifier (E&I 2100 L) and a signal generator (GI 5100 L). The resonance frequency of the system was 42.2 kHz and the power set was a net electrical power of 8 W. Some experiments were recorded with a high speed color camera (48 MP (Sony IMX586) in One Plus 7 pro @ 240 fps) to study transformation of polymorphs during the process.

For flow crystallization experiments, the ROY-acetone solution and anti-solvent were pumped (Buchi pump Module C-601) through a flow crystallizer. The crystallizer was custom made with a glass capillary channel (L = 10 cm, W = 0.7 cm and H = 700 µm) enclosed in a glass water bath for temperature control (see Fig. 1b). Figure 1c shows the schematic of the flow experiment. The total flow rate (TFR) was kept constant when varying the anti-solvent VF. Experiments were conducted at two TFRs of 2.5 mL/min and 10 mL/min. These correspond to Reynolds numbers (Re) of 10.4 and 41.6, and Peclet numbers (Pe) of 93.3 and 373, respectively. Because of the low Re and high Pe number, the flow was in the laminar regime in both cases and the mixing was dominated by convection. This also emphasizes the scope for using ultrasound for additional mixing. The residence time for a flowrate of 2.5 mL/min was 12 s, while for a flowrate of 10 mL/min this was 3 s. VFs of 0.2, 0.4 and 0.85 were tested in each case. The outgoing suspension was filtered using a vacuum filtration setup with 0.22 µm filter. The crystallizer was attached to an ultrasonic transducer (Steminc -SMBLTD45F40H) to enable sonicated experiments. The resonance frequency of the system was found to be 39.3 kHz. The net power was limited to 3 W (± 1 W) to avoid damage to the glass crystallizer. A Photron Fastcam mini UX100 high speed camera with a Navitar 12x zoom lens (12 mm FF) was used to analyze fragmentation.

In this work, ATR-FTIR was used for characterizing the polymorphs more reliably rather than depending only on the microscope. Reference spectra of yellow prisms, red prisms and orange needles were made using either the commercial product or pure product from crystallization experiments. A light microscope (Motic BA400) was also used for imaging the crystals and further characterization. Raman spectroscopy was tried

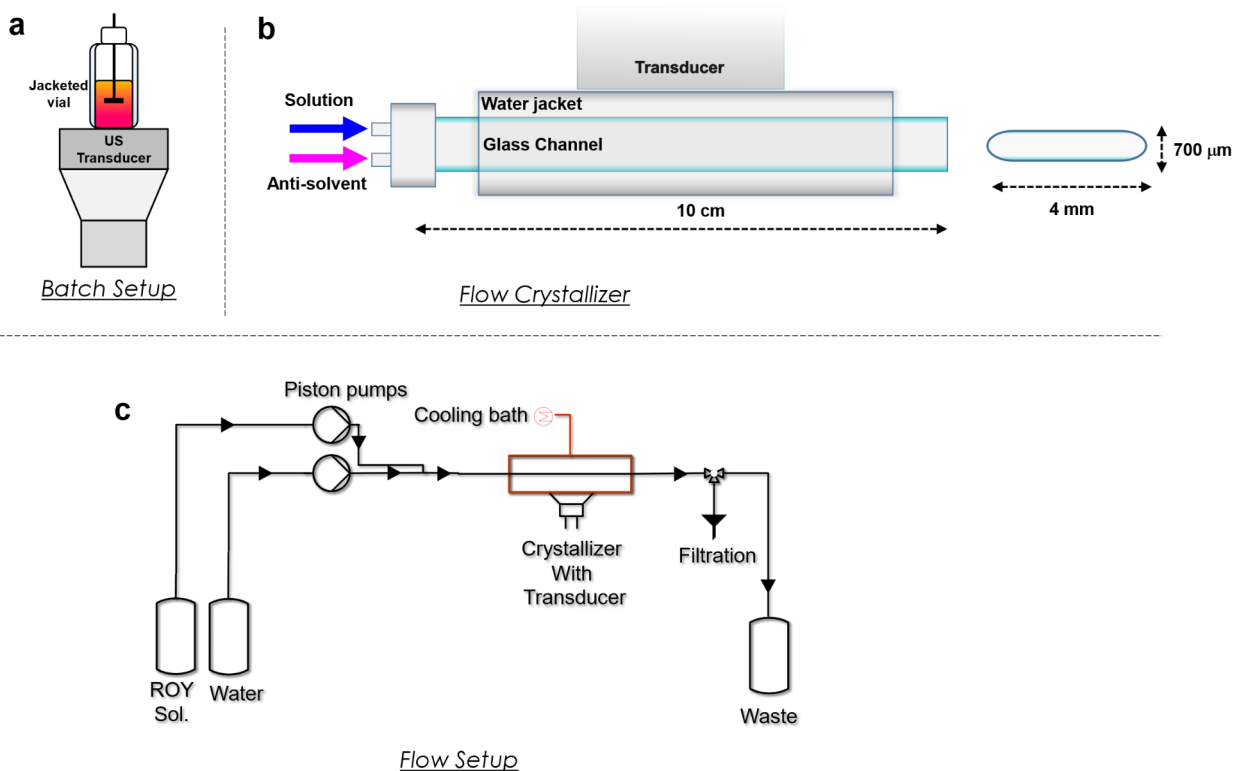


**Fig. 1.** (a) Schematic of the batch experimental setup. (b) Schematic of the flow crystallizer. (c) Schematic of the flow crystallization experimental setup.

as well for analyzing these crystals, however, fluorescence of the sample hindered in getting reliable peaks for characterization. Induction time and yield are also measured. Induction time is considered as the time at which the first crystals are observed since the starting point of the experiment in both batch and flow crystallization schemes. Yield represents the ratio of the crystallized mass over the supplied mass of the solute. In flow experiments the flow rate and collection time are taken in to account when determining the supplied mass of the solute.

### Computational fluid dynamics (CFD)

A CFD study was conducted to get a broad idea of the distribution of solution and anti-solvent in the channels before nucleation. This analysis was limited to silent conditions for simplicity. The study was conducted using COMSOL Multiphysics package (version 6) which is a finite element method based software. The linear, incompressible, time dependent, 3D, Navier-Stokes equations were coupled with transport of species equations to solve the distribution of the solution and anti-solvent species. At the boundaries, one inlet of the channel was specified as the ROY solution and the second was specified as water. Velocity boundary conditions were specified at the inlets and a zero-pressure boundary condition was specified at the outlet. No slip boundary condition was specified for the walls. A tetrahedral mesh with 14 million elements was used. The resultant species distribution was used to estimate the spatial supersaturation profile in the system. The results were then correlated with the experiments to better understand the relation between supersaturation and nucleated polymorph.

For experimental validation, a separate setup with the same glass channel used in flow crystallization experiments, having a Y inlet was used. It was placed flat under a mini microscope (KK Moon 1080p mini microscope) for recording. The mini microscope was panned over the length of the channel during the experiment. Experiments were conducted using a dye (Rose Bengal) mixed in the solvent – acetone for one inlet and water for the other inlet. The color distribution was recorded with the microscope over the length of the channel. This distribution was quantified by extracting the pixel color intensity using a *python* code (*Pillow* module). This data was used for experimentally validating the simulation results. This approach is similar to the work in<sup>14–16</sup>. Figure S1 in the Supplementary Information shows the comparison of the experimental and simulation results. The practical factors in experimental data like surface reflections can cause some discrepancies but the results seem to be generally in agreement. These simulations were used to obtain a reliable approximation of the areas where supersaturation levels are likely to be high.

### Cavitation analysis

Acoustic cavitation is dependent on the ultrasonic frequency, ultrasonic power, the fluid medium and crystallizer geometry<sup>6</sup>. It is important to confirm the presence of acoustic cavitation to correlate the observed results. This

was done using sonochemiluminescence experiments. A 10 mM luminol (3-aminophthalhydrazide (98% TCH/Fluka chemicals) solution was prepared in DI water. 0.84 g of NaOH (>97% Sigma Aldrich or Alfa Aesar) was added to 200 mL solution to bring the pH to 12. Experiments were conducted for both the batch and the flow crystallizers, where in the luminol solution was added to the vial or the channel or the bath enclosing the channel and then sonicated. The luminescence was recorded using a Nikon Z6 II digital camera, with a NIKKOR lens (focal length 105 mm) in a dark environment. In all experiments the added luminol solution was kept stationary as ultrasound was applied.

## Results

### Batch experiments

Batch crystallization experiments were conducted with solutions of 50 mg/mL starting concentration. The anti-solvent VFs of 0.2, 0.4 and 0.85 were used. The experiment was observed for a duration of 60 s. Experiments without ultrasound were conducted first. For reproducibility, experiments were conducted 3 times for each condition at least.

In previous literature only light microscope was used for characterizing the polymorphs<sup>11</sup>. Due to the limited sample size ( $\approx 100$  mg) and the possibility of crystals being densely packed on top of each other, a more reliable technique was needed. ATR-FTIR was found to be a good solution which allowed immediate analysis of the product. This is especially useful for microfluidic flow crystallization where throughput can be low. For determining standard spectra of each polymorph, the sample used was first screened thoroughly using light microscopy. When it was confirmed that the solids consisted of an exclusive polymorphic form, this sample was then analyzed by FTIR to determine its spectra. The pure commercial ROY was identified under light microscopy as R (Red prisms), while Y (Yellow prisms) were found after crystallization experiments. ON (Orange needles) were found after evaporative crystallization of ROY. Using these samples R, Y and ON could be standardized. From the FTIR spectra of these polymorphs, two different regions of wavenumbers were found to be of interest:  $3320\text{ cm}^{-1} - 3270\text{ cm}^{-1}$  and  $850\text{ cm}^{-1} - 820\text{ cm}^{-1}$ . R has a peak at  $3305\text{ cm}^{-1}$  while the peaks for Y and ON were shifted to  $3281\text{ cm}^{-1}$  and  $3284\text{ cm}^{-1}$  respectively. ON also has a peak at  $847\text{ cm}^{-1}$ , whereas Y has a peak at  $840\text{ cm}^{-1}$  while R has a small peak at  $832\text{ cm}^{-1}$ . The standard spectra of OP (Orange Plates) and YN (Yellow needles) was not determined since it was not possible to isolate the crystals. However, it was noticed from the experiments that the spectrum of OP was quite similar to that of R. The result is always judged by a combination of both FTIR and light microscopy for better reliability.

Coming to the results of crystallization experiments, it was found that at 0.2 VF, silent condition, the product consisted solely of the Y polymorph which is the most stable form<sup>17</sup>. This agrees with what has been found in literature<sup>11</sup>. When the system was sonicated, the outcome remained the same i.e., Y. Figure 2 shows the FTIR

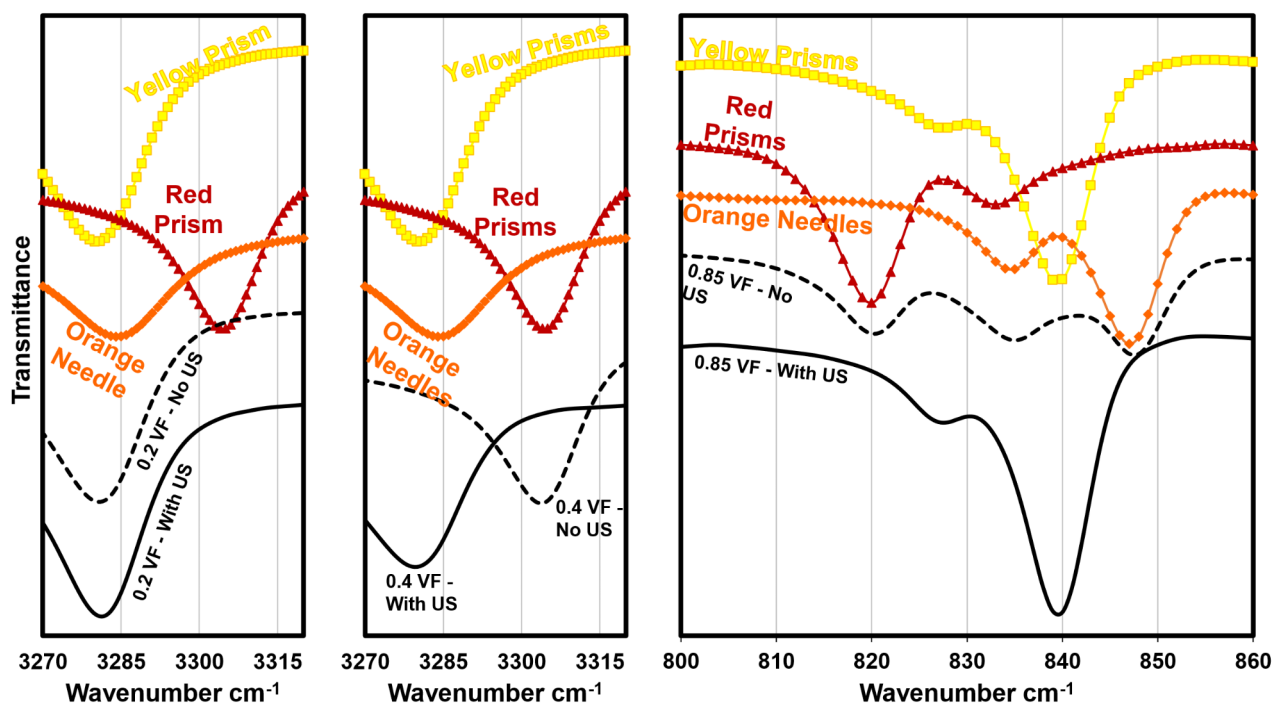


**Fig. 2.** ATR-FTIR results for batch experiments at different anti-solvent VFs. Colored curves show reference spectra of the indicated polymorphs – Yellow prisms (Y), Red prisms (R) and Orange needles (ON). US – Ultrasound.

spectra while Fig. 3 shows the microscope images. For experiments at 0.4 VF, the product in silent conditions was a combination of OP, Y and very small traces of ON, with an abundance of OP. It was possible here that the presence of Y in the crystallization experiments at 0.4 VF could also be a result of transformation rather than nucleation. According to Ostwald's rule, which states that first the metastable polymorphs will crystallize and afterwards transform into the stable polymorph, OP will crystallize initially and may then transform into Y<sup>18</sup>. When the same experiment was conducted with sonication the product completely consisted of the Y polymorph. A similar result as seen by Nerom et al.<sup>13</sup> where improved mixing (by conventional methods and

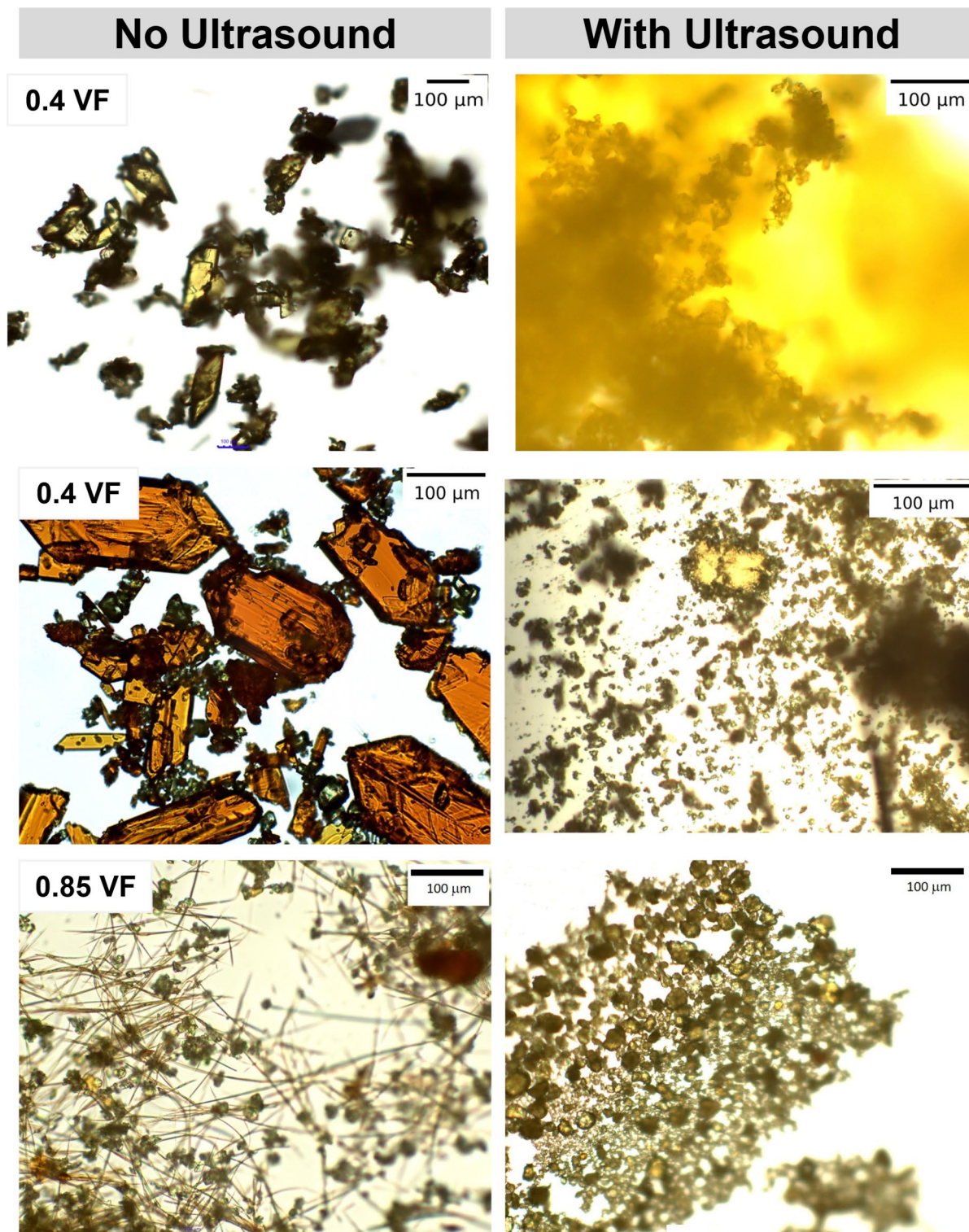


**Fig. 3.** Microscope images of the filtered crystals from batch crystallization experiments.

acoustic streaming at 1 MHz) led to change in polymorph for ROY. It is, however, important here to further investigate the mechanism which could be twofold in light of the presence of acoustic cavitation. First, due to mixing and cavitation inside the channel, supersaturation could homogenize and Y could nucleate<sup>19</sup>. The second possible reason could be transformation of other forms to the stable Y form. Transformation could again be enhanced due to the effects of ultrasound such as mixing and local high temperatures. In our experiments it is visually observed that the color of the contents in the crystallizer begins with orange and then changes to yellow indicating a contribution of transformation. This is investigated further in detail in the next section.

For experiments conducted at the highest VF of 0.85 in silent conditions, a mixture of Y, OP and ON was found, with an abundance of ON. The FTIR standard spectra in the region of  $3320\text{ cm}^{-1}$  to  $3270\text{ cm}^{-1}$  for 0.85 VF compared to the standard spectra of R, Y and ON can be seen in Fig. 2. The mixture of polymorphic form can be explained due to the stability of the polymorphs. Due to the higher supersaturation, OP and ON will crystallize faster than the more stable Y polymorph. The presence of Y again can either be due to direct nucleation after the supersaturation depletes (due to ON and OP nucleation) or a transformation of ON and OP during the process. Similar to what was seen at 0.4 VF, when the same experiment was conducted with sonication the product consisted only of the Y polymorph. Ultrasound favoring the most stable form was also observed in previous research for e.g., in the case of *p*-ABA as observed by Gracin et al.<sup>9</sup>. The local hotspots from acoustic cavitation could result in sufficiently high temperatures to increase the solubility such that the previously formed crystals were able to redissolve and transform into the more stable polymorph.

Looking at the induction times, which could be extracted precisely from the high speed recordings of the experiments, a decreasing trend with increasing VF and with sonication can be noticed (see Fig. 4). For a VF of 0.2, when water was added, emulsions were formed within the fluid mixture in the crystallizer. This phenomenon is called oiling out. Oiling out should be avoided in crystallization since the oil phase is a good solvent for impurities<sup>20</sup>. This will lower the purity grade of the end product. Oiling out is mostly observed when crystallization is kinetically hindered. The oiling out of the water inside the ROY solution affected the induction time. The oil emulsions first had to be destabilized such that the water could mix with the ROY solution. The induction time for 0.2 VF was found to be an average of 10 s. The experiments also showed that once crystallization started this would lead to the destabilization of the still existing emulsions. The effect of oiling out also decreases with increase in VF and crystallization could occur sooner. The induction time in the case of 0.4 and 0.85 VF was within 3 s.

Ultrasound is, generally, known to reduce induction times since the presence of cavitation enhances nucleation rates<sup>21</sup>. The induction time for 0.2 VF decreased to an average of 7 s which is about 30% lower compared to the silent case. The induction time for the 0.4 VF and 0.85 VF was not altered much since the crystallization occurred already at less than 3 s. In addition to better mixing of the system, ultrasound was also quite effective in reducing the effect of oiling out and thereby also enabling faster nucleation. As for yield of the experiments, application of ultrasound resulted in an increase in yield. The yield for silent conditions at 0.2, 0.4 and 0.85 VF was an average of 14, 22 and 23% of the mass of crystals dissolved. This increased to an average of 21, 43 and 46% with ultrasound, respectively.

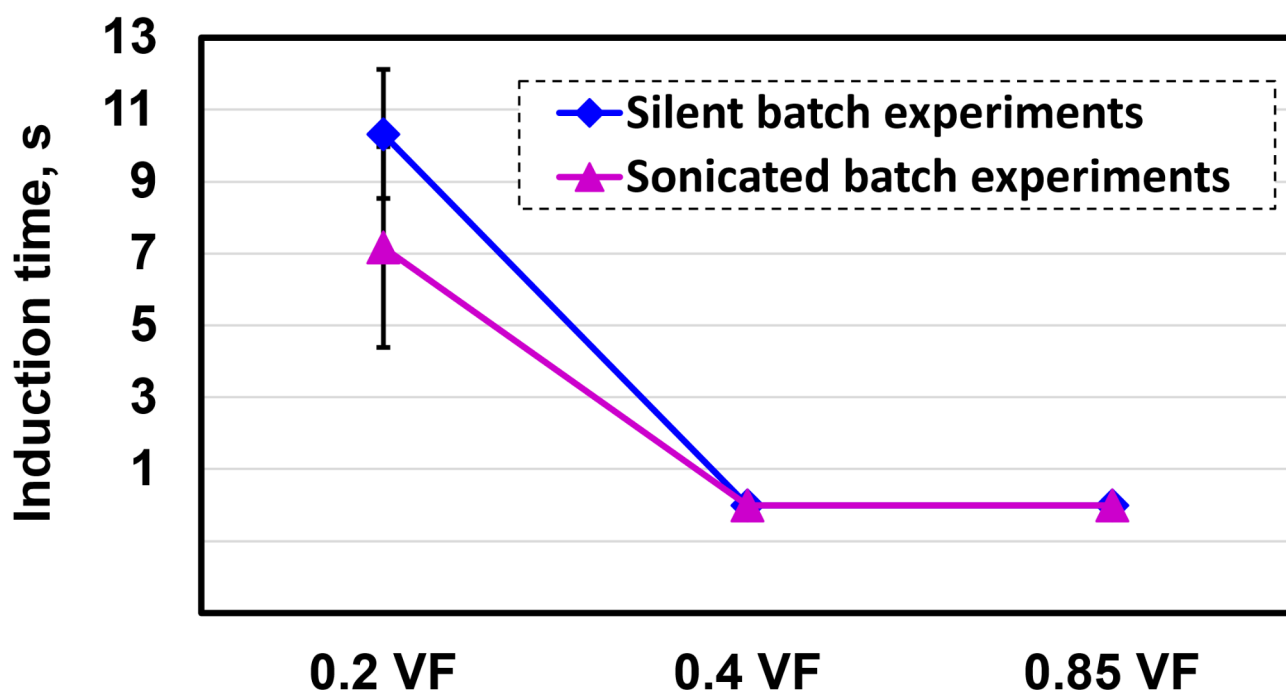


Fig. 4. Induction times of the batch crystallization experiments.

### Transformation study

The nucleation and transformation of the ROY polymorphs is a quick process which can occur within a minute. This makes it difficult to extract samples from the system for external analysis. Additionally, the process of extraction or any in-situ probe can also affect the crystallization process, affecting the reliability of any such experiment. The special aspect of color differences between the polymorphs of ROY can be used to one's advantage here to track the transformation. Therefore, to probe the extent of transformation versus nucleation during crystallization, both silent and sonicated experiments were recorded with a high speed color camera to capture the change from orange to yellow over the duration of the experiment. This change was measured by tracking the variation in the green component of the pixels of the crystallizer from the recorded frame. The green component value is averaged for all pixels of the crystallizer area per frame to mitigate the effect of increase in color intensity due to higher yield. Figure 5 (a) shows an example image of the crystallizer at the onset of crystallization showing orange color and at the end of the experiment showing color changed to yellow. Figure 5 (b) shows the average green color intensity over the experiment duration (AGCI) for three identical experiments under both silent and sonicated conditions (at VFs of 0.2, 0.4 and 0.85). Each AGCI curve must be considered independently to notice the difference in intensity over time rather than comparing the absolute values between different curves.

For the experiments at 0.2 VF the AGCI remains similar for both silent and sonicated conditions. This is because, in both cases Y polymorph crystallizes immediately, there is no scope for transformation hence there is no change in the color intensity over time. For the experiments at 0.4 VF a significant increase in AGCI over time can be seen. The silent experiments show a gradual increase in AGCI, while the sonicated experiments have a sharp increase. The silent experiments can be divided into four different intervals. The first interval, from 0 to 2 s, is the addition of water into the crystallizer, which lowers the average color intensity because of the filling of the analyzed volume. The second interval, from 2 to 10 s for the first and second experiment and 2–15 s for the third experiment, has a slight increase in AGCI. This slight increase can be explained by the increase of solids inside the crystallizer (crystallization period). The third interval, 10–15 s for the first experiment, 10–20 s for the second experiment and 15–22 s for the third experiment, has a sharp increase in AGCI. This sharp increase is due to the transformation of OP into Y. The last interval, from 15 to 60 s, 20–60 s and 22–60 s for the first, second and third experiment respectively, shows a stagnation of AGCI. From this point on the transformation had stopped. The sonicated experiments can be divided in similar intervals. The first interval, 0–2 s, is again the addition of water which gives a sharp decrease in average color intensity. The second interval, 2–10 s for the three experiments, shows a sharp increase in AGCI which flattens afterwards. This is the period of nucleation of OP and followed by transformation to Y. Here the steeper increase in AGCI as compared to the silent experiments clearly indicates faster transformation with sonication. The last interval, 10–60 s for all three experiments, shows a constant AGCI indicating equilibrium of transformation. The transformation to Y initializes on average 8 s earlier for sonicated experiments as compared to silent conditions. Further information is provided in the Supplementary Information along with Figure S2, which shows a microscope image of the crystals taken 3 s after sonicated crystallization to confirm the polymorphic form.

The results for 0.85 VF show the most drastic difference in color intensity behavior between silent and sonicated experiments. The results can be seen in Fig. 5. The color intensity change in silent experiments can be divided into three intervals. The first is the initial drop in AGCI from 0 to 3 s due to the addition of the anti-solvent. The next interval is representative of the concomitant crystallization of OP and ON, which can be seen as the plateau in the figure from 3 to 12 s. There is no increase in AGCI due to the crystallization being immediate. The last interval, 12–60 s, a slight increase of AGCI can be observed which is characteristic of transformation. The sonicated experiments can again be divided into three intervals, same as those of the silent experiments. From 0 to 3 s is the addition of anti-solvent into the system, which is the first interval. This gives a sharp drop in AGCI. The second interval lasts from 3 to 8 s which represents the concomitant crystallization of OP and ON. Following this one can see a sharp increase in average color intensity. This increase then begins to slow down but does not completely stabilize, which is the third interval lasting from 8 to 50 s. This interval is the proof that the occurrence of Y polymorph in the product is a result of OP and ON transformation. One can notice here that in the silent case the transformation is not as steep as compared to the silent case at 0.4 VF. This is because of the supersaturation being much higher at 0.85 VF than at 0.4 VF which hinders the transformation. This, however, is not a hindrance in the sonicated case where a steep transformation curve can be seen.

### Flow experiments at 2.5 mL/min

The silent experiments with a flowrate of 2.5 mL/min showed that for 0.2 VF the product consists of OP instead of the Y polymorph, which is contrary to the batch experiments. This could be a result of a difference in mixing inside the flow crystallizer as compared to that in the batch crystallizer. Due to the low Peclet number there could be sub-optimal diffusion of the solution and anti-solvent creating an interface between the two fluids which could result in an inhomogeneous supersaturation. Oiling out was also observed in these conditions. Figure S3 in the supplementary information shows a picture inside the crystallizer. The OP and the oil emulsions can be clearly seen. When the product was analyzed by light microscopy, as can be seen in Fig. 6, for the 0.2 VF flow experiments, a combination of R, OP, Y and some ON was found. This was then confirmed by FTIR analysis as seen in Fig. 7. When ultrasound was applied, there was a decrease in induction time and a reduction of the oiling out effect. Furthermore, there was a change in polymorphic form similar to what was seen in the batch experiments. Instead of the product consisting mainly out of OP as in the silent experiments, the product was now mostly the Y polymorph with some OP. Ultrasound and the resultant cavitation seemed to improve the uniformity of the anti-solvent in the system and provide better conditions for the Y polymorph to form. It is again probable that the OP would transform into Y inside the crystallizer because of the applied ultrasonic conditions.

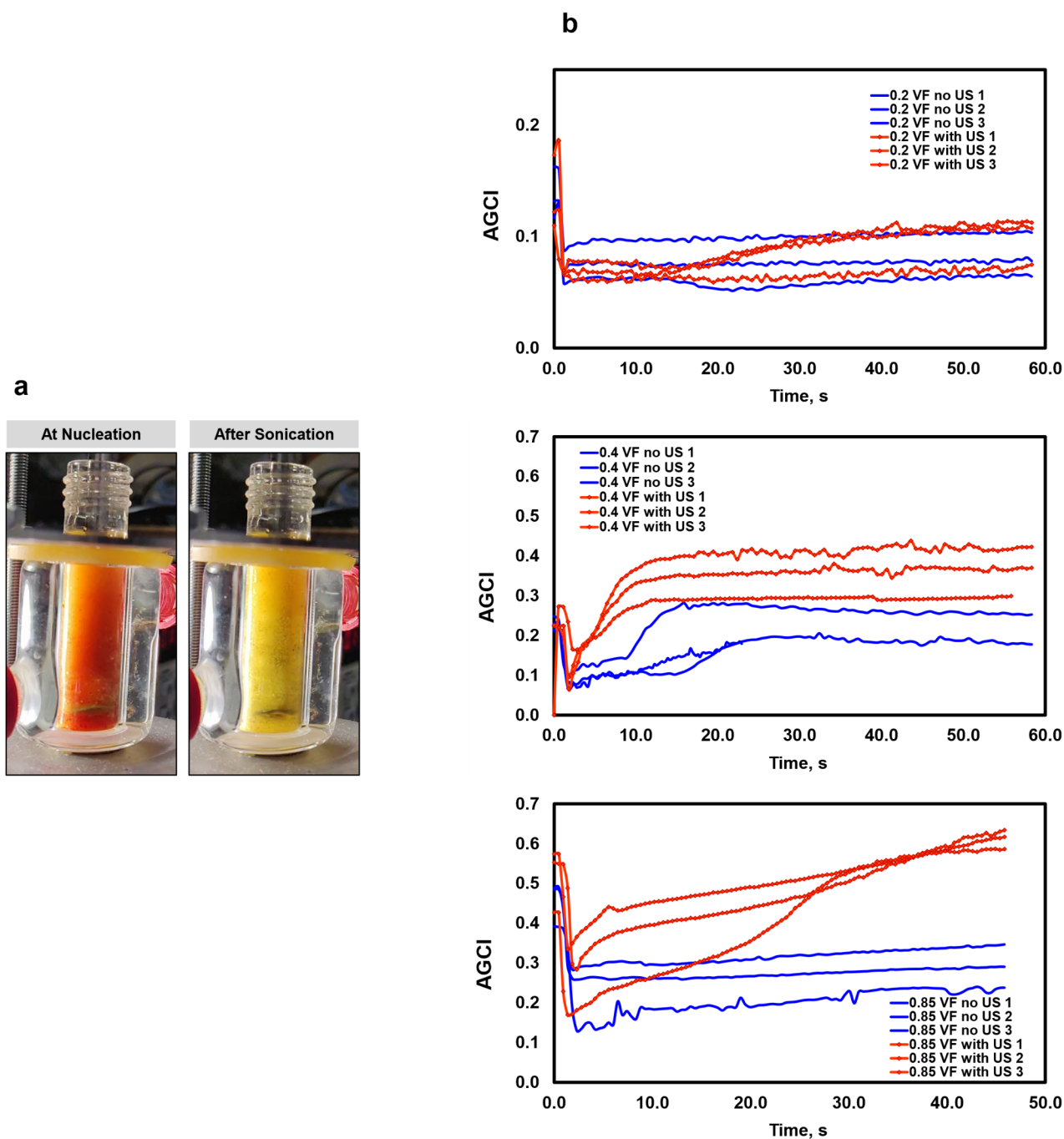


**Fig. 5.** Transformation analysis in batch crystallization experiments (a) Example picture showing complete transformation of ON to Y in the crystallizer at 0.85 VF with ultrasound. (b) Average Green Color Intensity change (AGCI) over time to track the change in color from orange to yellow in the triplicate experiments at different VFs. US – Ultrasound.

For a VF of 0.4 the product consisted of OP and ON, with OP being the dominant polymorph in silent conditions. Again, the contrast with batch experiments is the absence of Y polymorph in the product. This can be explained due to the continuity of the flow experiments. The difference with the batch experiments is that after crystallization of OP the supersaturation lowers which either helps nucleation of, or transformation to, the Y form. This is not the case for the flow experiments since the solutions keep getting replenished over time. The product mixture of OP, R, ON and Y with an abundance of OP were confirmed by microscopy and FTIR. When ultrasound was applied, again it was apparent that the polymorphic outcome was different since the product was now a mixture of abundantly Y with some R.

In the case of 0.85 VF, a lot of different polymorphs were found in the silent conditions. There was substantial clogging in the channel. There was nucleation of the needle like polymorphs which would lead to clogging of

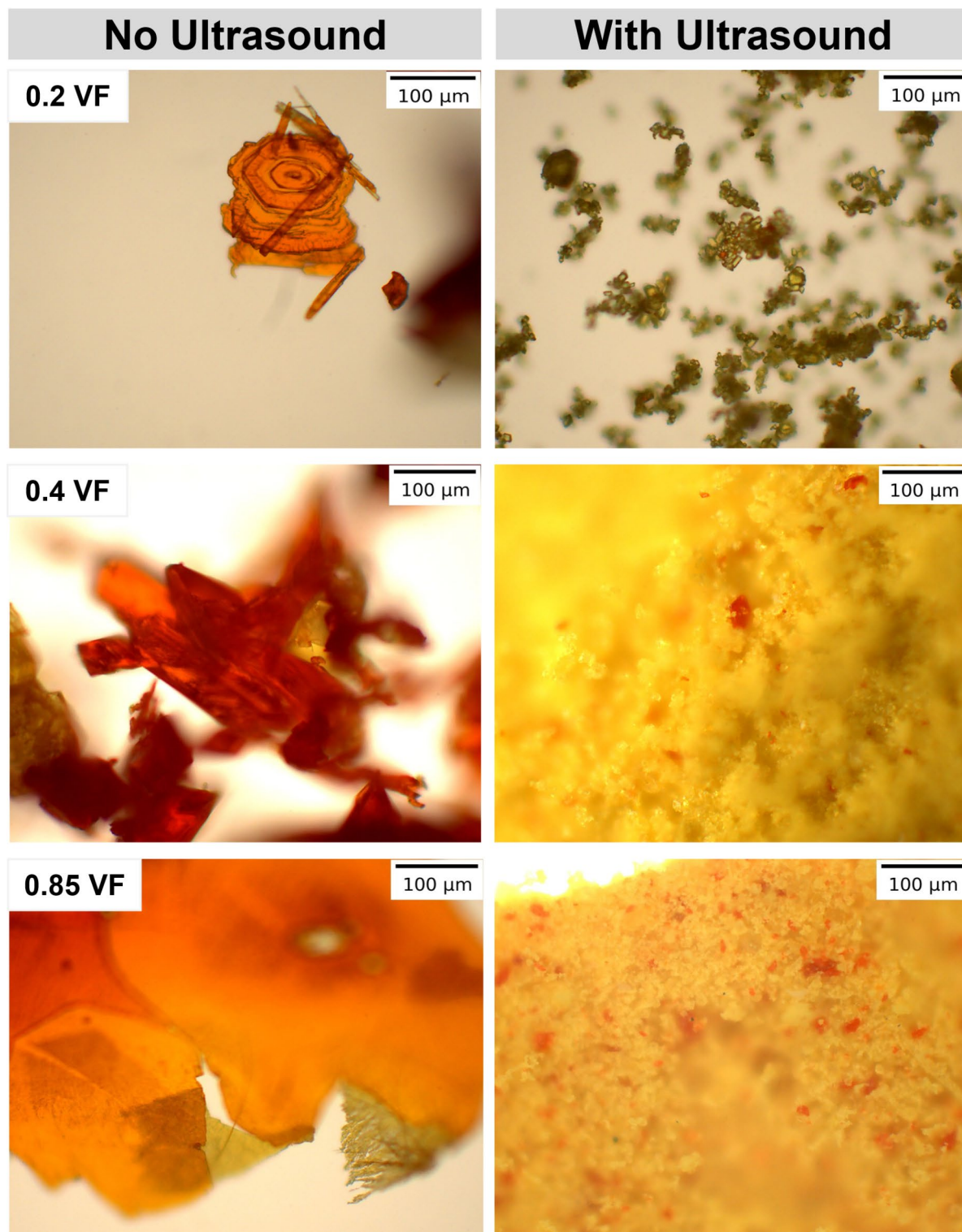


**Fig. 6.** Microscope images of the filtered crystals from flow crystallization experiments at 2.5 mL/min.

the channel. Due to clogging sometimes it was difficult for all crystals to flow out. Hence the collected product did not represent all the formed crystals. FTIR and light microscopy analysis of collected product show presence of mainly YN and ON. The polymorphs found in the product again changed when the system was sonicated. The resulting polymorphs were Y and traces of R. This is again expected to be a result of cavitation/mixing enhanced transformation within the channel. Apart from temperature effects cavitation could also enhance transformation by fragmenting the crystals which makes them easy to dissolve in the solution. In order to test this, some basic, qualitative experiments were conducted in the flow channel which do indicate the possibility

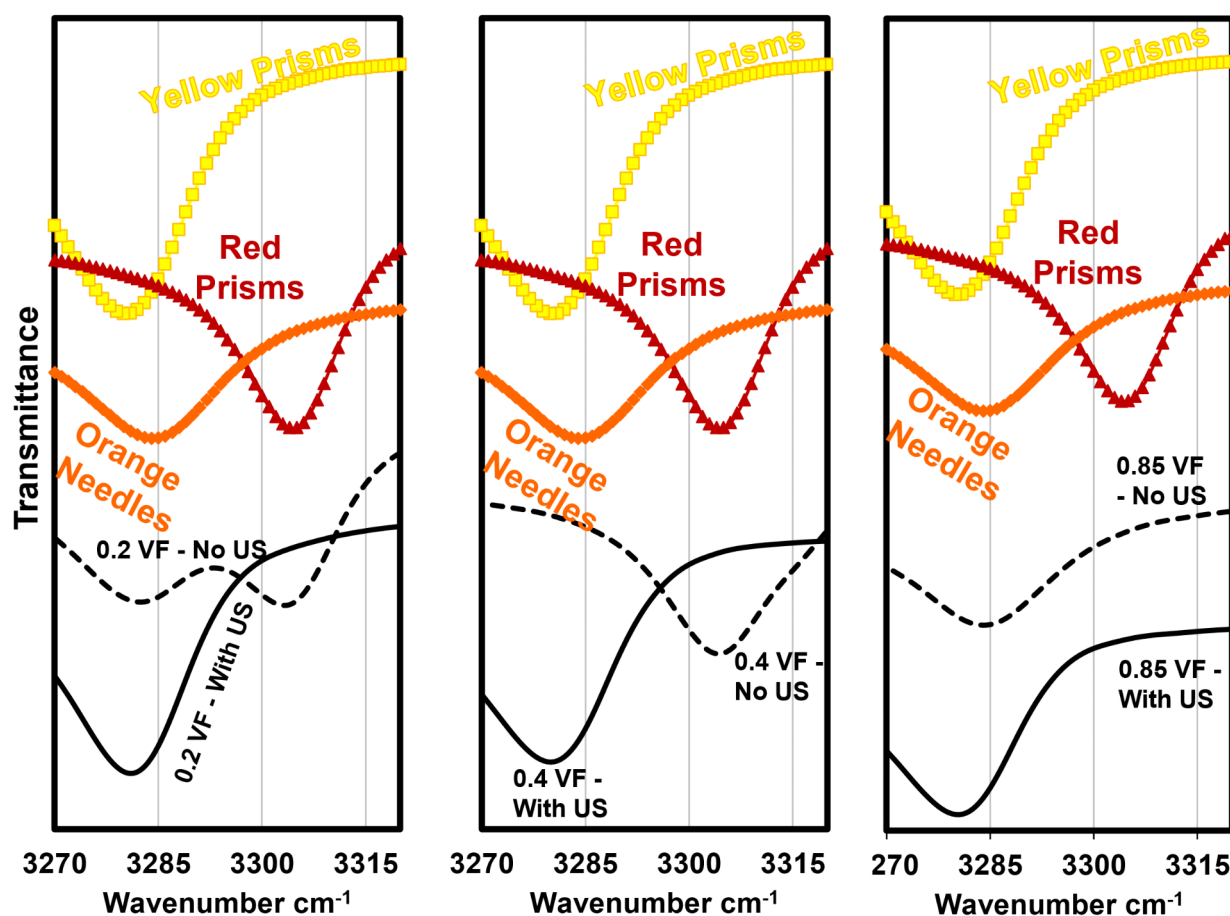


**Fig. 7.** ATR-FTIR results for flow experiments at 2.5 mL/min for different anti-solvent VFs. Colored curves show reference spectra of the indicated polymorphs – Yellow Prisms (Y), Red prisms (R) and Orange needle (ON). US – Ultrasound.

of fragmentation due to the cavitation at these ultrasonic conditions. These results are presented in Figure S4 in the Supplementary Information.

#### Flow experiments at 10 mL/min

Raising the flowrate could help increase mixing, which can have an effect on the polymorphs, induction time and the yield. Simultaneously, the residence time goes down (from 12 s to 3 s), which can also have its effect on the polymorph transformation time. The combined effect led to results quite different from the case of 2.5 mL/min. At 0.2 VF, the first observation was that the oiling out effect was significantly diminished. In the silent case, the polymorphic outcome was a mixture of a wide array of polymorphs. While for 2.5 mL/min the product was a mixture of mainly OP with other polymorphs at this VF, at 10 mL/min the product was a mixture of OP, R, YN, ON and Y with significant proportions (see Figs. 8 and 9). With ultrasound, the polymorphic outcome changed again. The product was a mixture of mainly Y with R and OP. The needle-like polymorphs YN and ON were now unable to form due to the effects of ultrasound. However, compared to the flowrate at 2.5 mL/min what is most remarkable is the higher concentration of OP and the presence of R in the product (observed in microscope images). This could probably be because of the low residence time which hinders complete transformation into the Y form.

The product for the silent experiments at 0.4 VF consisted of OP, R, ON, Y and YN. This is different to what was found for the flow experiments at 2.5 mL/min (0.4 VF) as YN were not present there. The product for the sonicated experiments at 0.4 VF was a mixture of R, OP and Y. This is a very different result from any sonicated experiment previously conducted. This is the first experiment in which R appeared in a high concentration. The product was expected to be consisting more of the Y polymorph as was the trend so far with ultrasound. The disappearance of YN and ON compared to the silent experiments at this flowrate and VF was not unlikely. The concentration of YN and ON were already low for the silent experiments and transformation could be expected when the system would be sonicated.

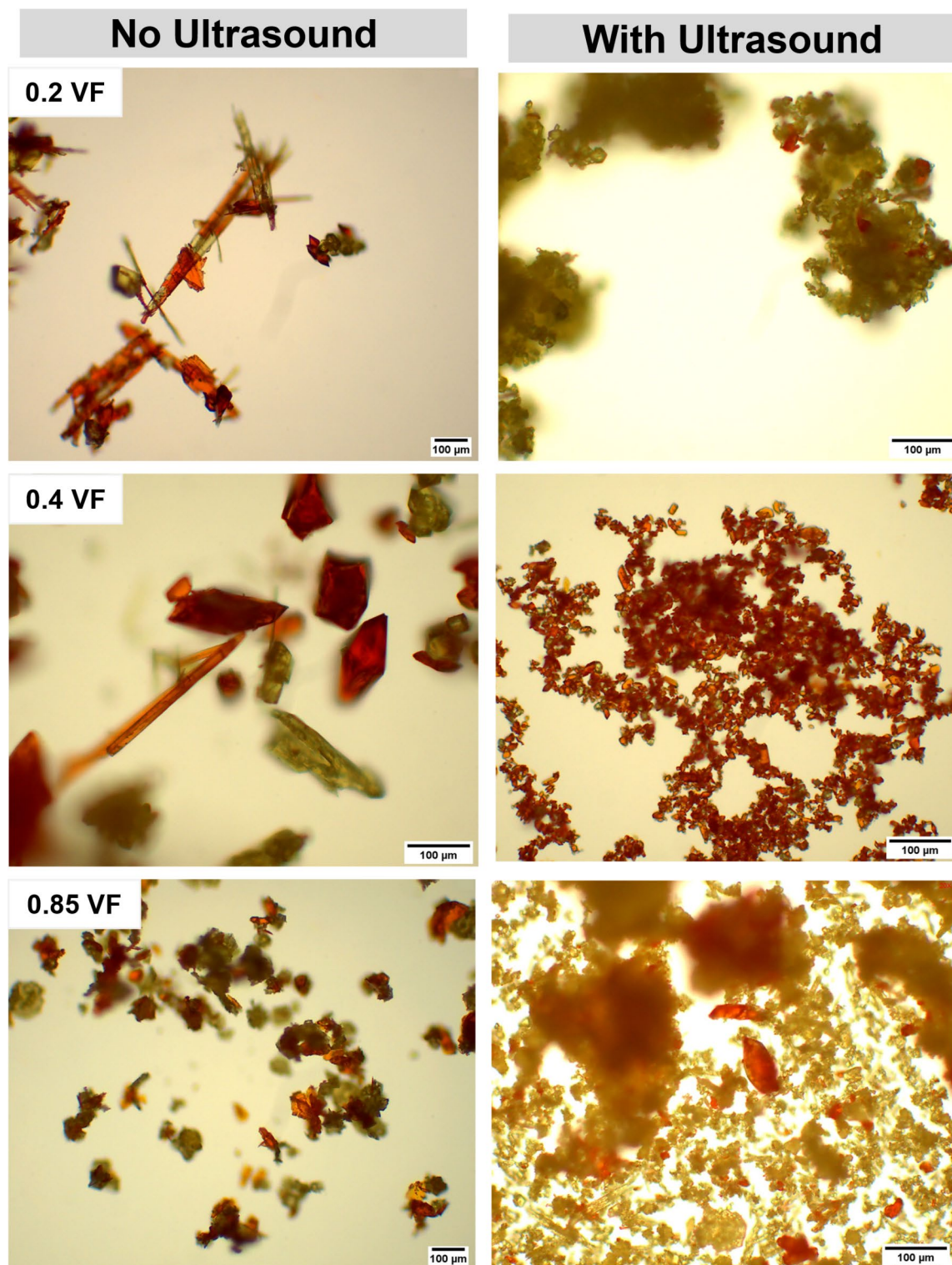


**Fig. 8.** Microscope images of the filtered crystals from flow crystallization experiments at 10 mL/min.

The product from the silent experiments at a VF of 0.85 consisted of a mixture of Y, R and OP. Again, this is very different from results at 2.5 mL/min. All silent experiments for a VF of 0.85 showed needles in their product, however, that was not the case at this flow rate. Furthermore, when sonicated a mixture of polymorphs was found. This mixture consisted out of Y, R, OP and YN. This is more in line with the experiments at a lower flow rate as the results found for the batch crystallizer. It shows again that when the system is sonicated the most stable polymorph forms. However, the main difference is the presence of YN. This is possibly due to high clogging that occurred at these conditions, even with ultrasound. Due to clogging local supersaturation

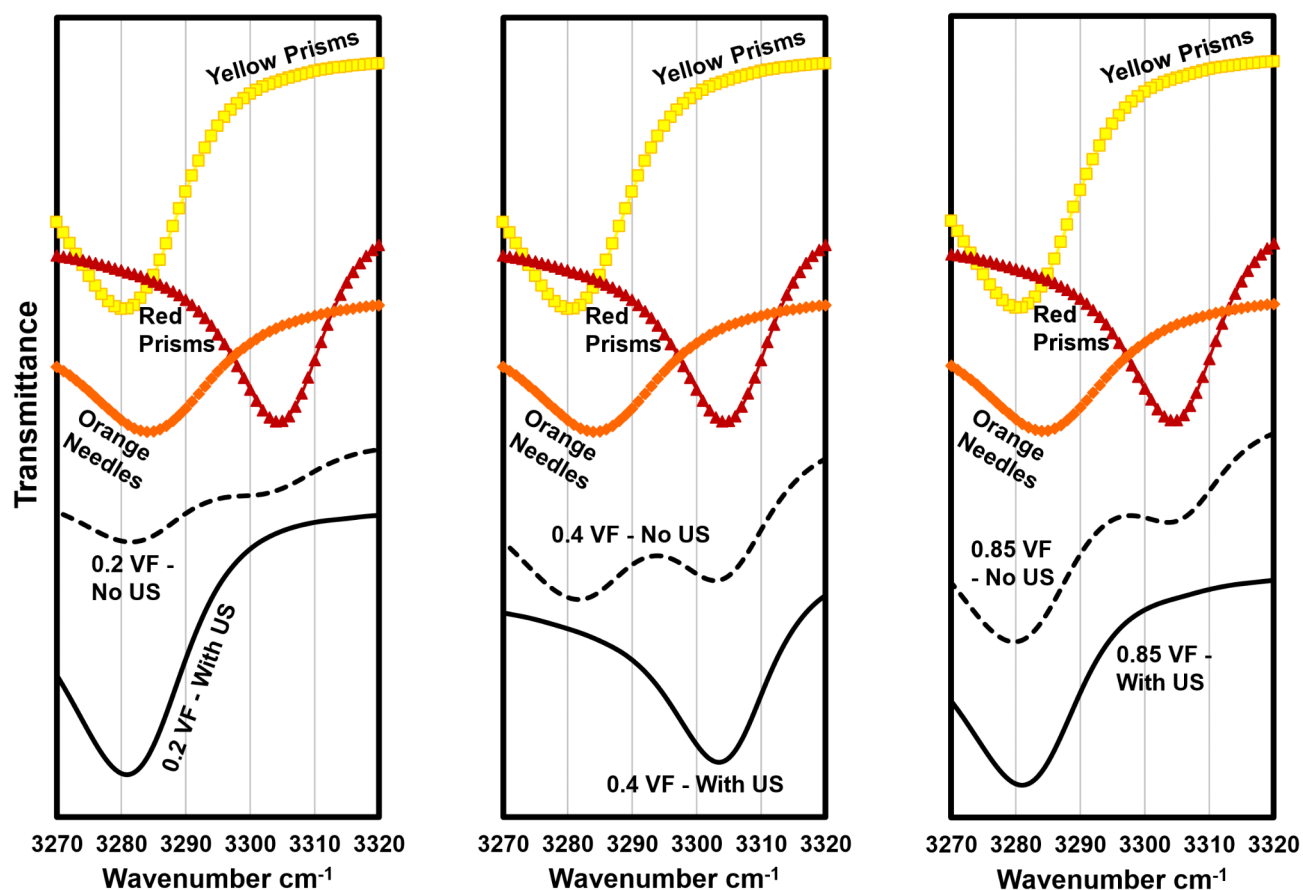


**Fig. 9.** ATR-FTIR results for flow experiments at 10 mL/min for different anti-solvent VFs. Colored curves show reference spectra of the indicated polymorphs – Yellow Prisms (Y), Red prisms (R) and Orange needle (ON). US – Ultrasound.

could further be disturbed. Stagnation around clogged areas led to nucleation of the needle-like polymorphs ON and YN. The lower residence time with this flow rate could also reduce any possible transformation of these metastable forms to the stable form before they exit the crystallizer. In general, the presence of clogging affected the polymorphic outcome at this VF for both silent and sonicated conditions.

As for induction times in flow crystallization, they decrease with an increase in VF and also when sonicated, similar to the result in batch experiments (see Fig. 10). When the induction times for both flow rates are compared, a decrease in induction time can be noticed with an increase in flow rate. In silent experiments for the flow rate of 2.5 mL/min the induction time decreased from an average of 108 s at 0.2 VF to 25 s at 0.85 VF. For 10 mL/min this decreased from 45 s to 6 s respectively. When ultrasound was applied for the case of 2.5 mL/min the induction time was 37 s at 0.2 VF and for higher VFs nucleation was immediate (< 3 s). For 10 mL/min the induction time reduced from 16 s to less than 3 s. In comparison with batch experiments, the induction times are higher for the silent case and for low VF of 0.2. This can be a result of the larger volume of the batch crystallizer which increases the chances of heterogeneous nucleation sources<sup>22</sup>. When ultrasound is applied for higher VFs the result is similar to the batch experiments i.e., nucleation is immediate.

The same effect of increase in yield with ultrasound was seen in flow experiments as well. The yield for flow experiments at 2.5 mL/min at 0.2 VF was an average of 10% which increased to 24.4% with ultrasound. For 10 mL/min the yield was similar. At 0.2 VF the yield was an average of 13% which increased to 21% with ultrasound. This is similar to that of the batch experiments at the same VF. For higher VFs occurrence of clogging affected the reliability of the quantities, hence they are not considered.

### CFD study

The conditions in a flow crystallizer channel before any nucleation occurs are crucial in determining the crystallization outcome. In flow crystallization, when there is no source of mixing, there can be distinct areas of high and low supersaturation within the channel. Experimentally this might be difficult to know in detail but tools like CFD can be used to model these conditions relatively easily. Hence, CFD simulations were conducted with the intended goal to model the conditions in the channel causing the first nucleation.

Figure 11 shows the result of the case of TFR 2.5 mL/min at 0.85 VF. Figure 11a shows the region being analyzed. Figure 11b shows the simulated distribution of the ROY solution in the channel from which a region in the channel where the supersaturation is between 2.03 and 7 is extracted as shown in Fig. 11c. Figure 11d shows a

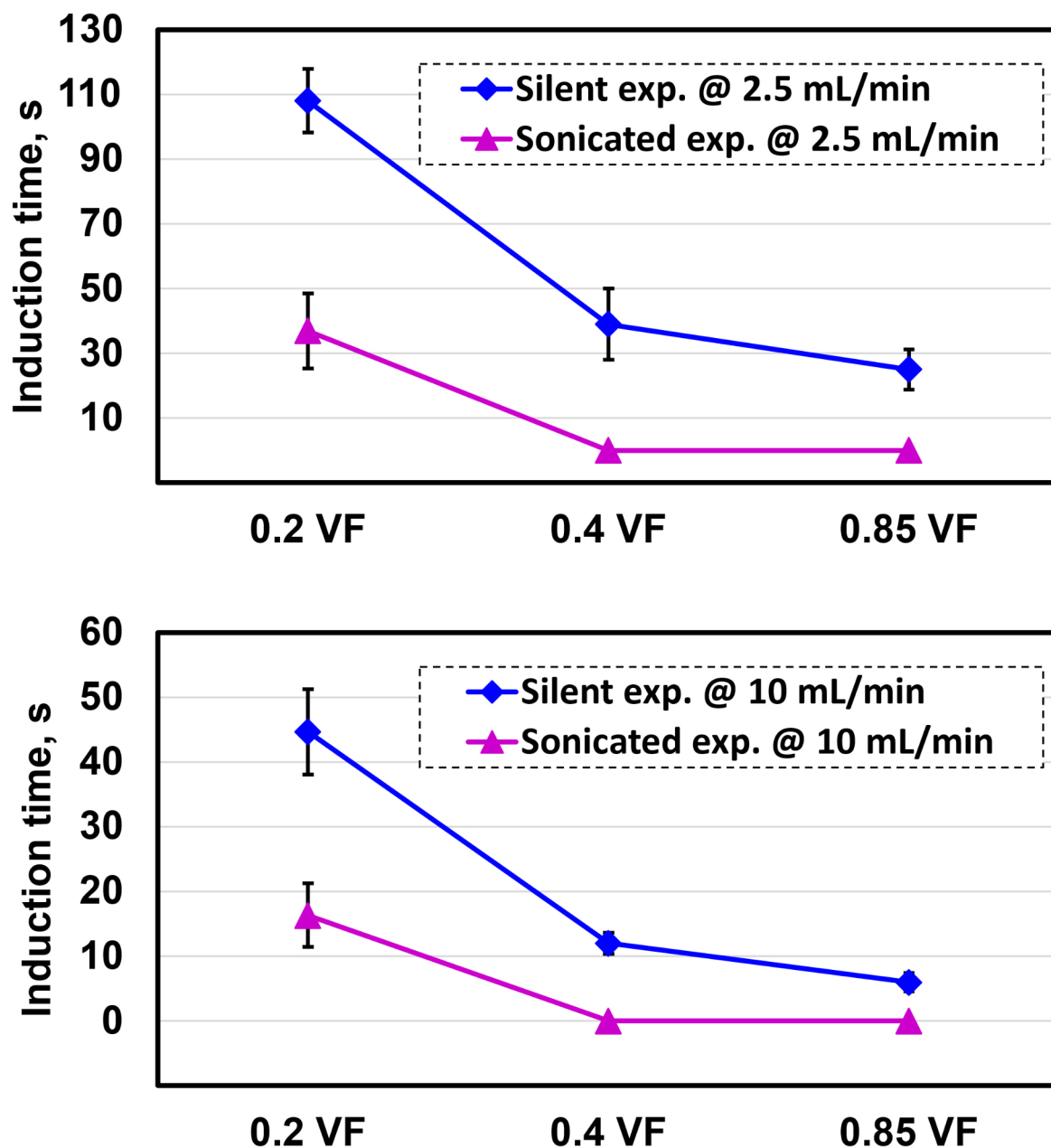
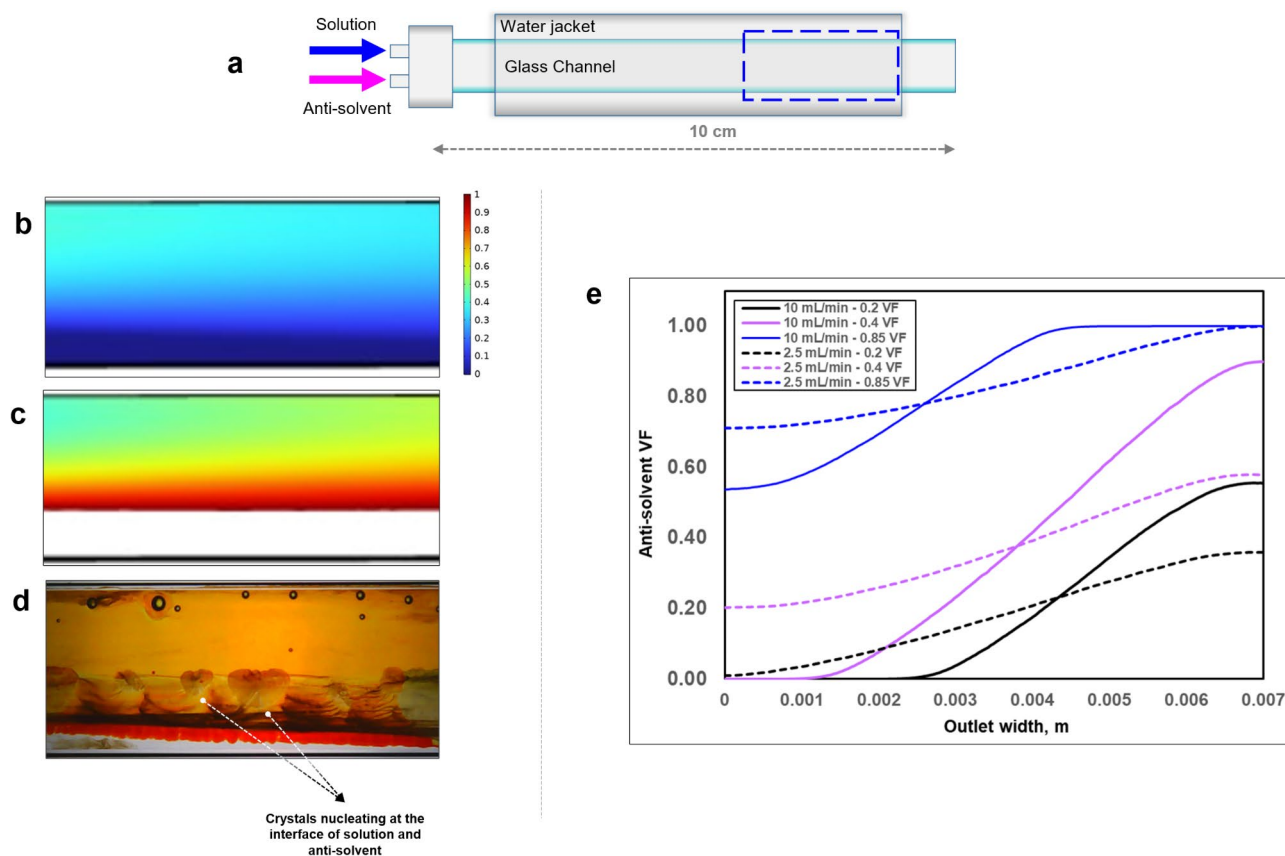


Fig. 10. Induction times recorded for flow crystallization experiments at different flow rates and VFs.

snapshot from the actual crystallization experiment where one can notice that the crystals nucleate in the region where the supersaturation is the highest. This indicates that the crystals in the flow channel in silent case nucleate at varying supersaturations due to lack of mixing and hence a variety of crystals are noticed. When ultrasound is applied this supersaturation inhomogeneity is reduced which gives way to either nucleation or transformation of the metastable polymorphs to the stable one. Further, a comparison was made of the anti-solvent VF at the outlet for 2.5 mL/min and 10 mL/min total flow rates at different inlet VFs (shown in Fig. 11e). Looking at the results one can observe that the lower flow rate of 2.5 mL/min allows a more smoother distribution compared to 10 mL/min. This can also explain the difference in polymorphic outcome seen in the experiments for these flow rates.

#### Sonochemiluminescence experiments

Sonochemiluminescence experiments were conducted in both the batch and flow crystallizers used for crystallization experiments. Considering the batch experiments first, the ultrasonic parameters used were same as those in the crystallization experiments i.e., a frequency of 42.2 kHz and a power of 8 W ( $\pm 2$  W). Results show that there was substantial luminescence in these conditions confirming the presence of transient acoustic cavitation<sup>23</sup>. Figure 12 shows the sonochemiluminescence results. Sonochemiluminescence was seen not just at the bottom of the crystallizer but also in regions further away and to the top of the crystallizer.



**Fig. 11.** (a) Showing region being analyzed. (b) Simulated ROY-solution volume fraction for 2.5 mL/min and 0.85 VF and  $t=60$ s. (c) Region between supersaturation of 2 and 7 extracted from simulation at  $t=60$ s. (d) Snapshot from the crystallization experiment showing crystallization occurring in a region where the supersaturation is high as seen in simulations. (e) Simulated anti-solvent VF at the outlet of the channels in the ROY experiments at different flow rates and inlet VFs.

The sonochemiluminescence experiments in the flow crystallizer were conducted in two ways. Firstly, the luminol solution was added only in the bath and not in the channel. Secondly, luminol solution was added only in the channel, and the bath was filled with water. This allowed to understand and differentiate the acoustic cavitation activity in the whole crystallizer versus the activity in only the channel. It was noticed, as shown in Fig. 13, that at the frequency of 39 kHz used with a power of 3 W ( $\pm 1$  W) there was substantial cavitation activity both in the bath and the channel. Looking at the larger picture of cavitation activity in the bath, it is clear that the cavitation is prominent around the center where the crystallizer is in contact with the transducer but does also exist substantially in the whole volume of the crystallizer. Since the design of the crystallizer is quite miniaturized, this allows for the cavitation activity to be present throughout the crystallizer. In comparison to the batch crystallizer, the calorimetric efficiency of the flow crystallizer is better since the calorimetric power of batch crystallizer was 0.047 W/mL at an applied power of 8 W whereas at the same applied power the calorimetric power of the flow crystallizer was 0.85 W/mL.

Looking at the results where luminol solution was added only in the channel, one can see that the cavitation activity occurs along the full length of the channel but, laterally, is localized near the edges of the channel. This could be due to the tendency of cavitation bubbles to heterogeneously nucleate along the edges of the channels and also due to the affinity of the coalesced cavitation bubbles to move towards the walls of the channels. The cavitation being present along the length of the channel is a positive aspect of the design as it enables uniform conditions during crystallization.

## Conclusions

In this work, anti-solvent crystallization of ROY was investigated under acoustic cavitation in batch and flow setups. In batch experiments, it was noticed that application of ultrasound resulted in a different polymorphic outcome as compared to the silent experiments. In silent conditions, experiments conducted at 0.2, 0.4 and 0.85 VF resulted in the product consisting mainly of Y, OP and ON. In sonicated experiments the product at all three VFs consisted mainly of the Y polymorph. There were two possibilities for this change. Firstly, direct nucleation of the Y prisms due to better mixing and cavitation bubble effects related to local thermodynamic conditions. Secondly, transformation of the nucleated metastable polymorphs like OP and ON in to the stable form Y facilitated again by better mixing and cavitation conditions. To study the extent of the transformation

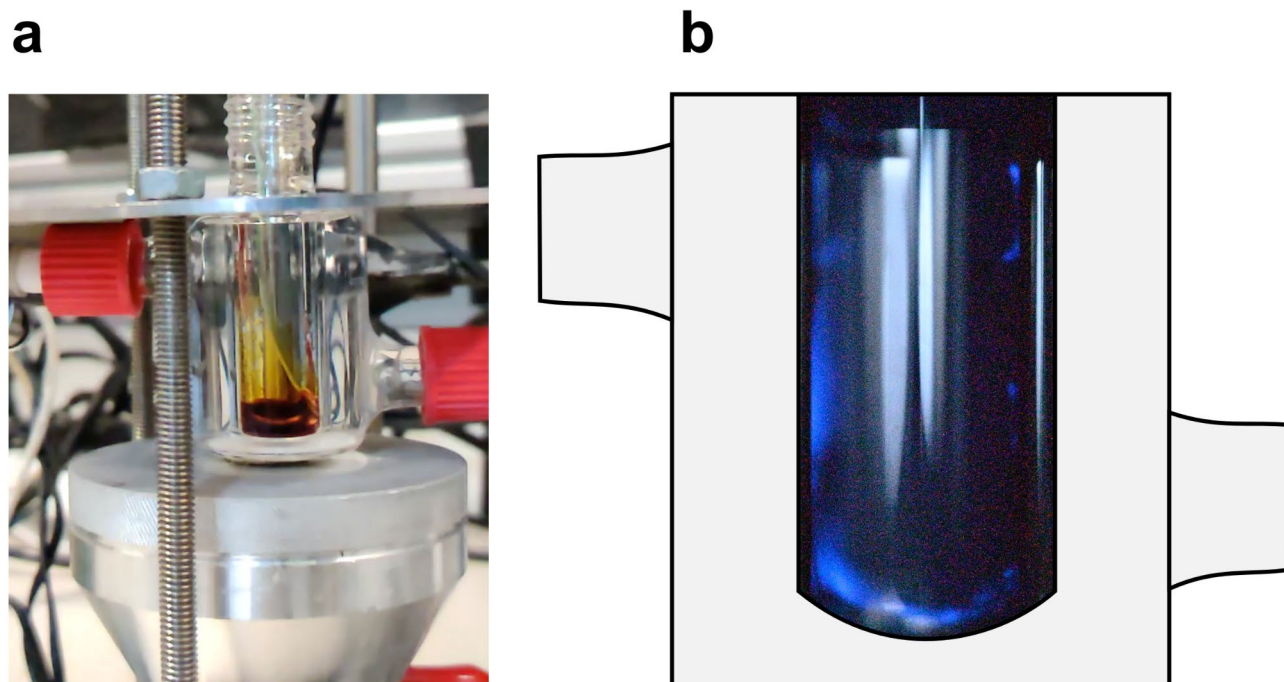


**Fig. 12.** Sonochemiluminescence in batch crystallizer used for ROY experiments. **(a)** Crystallizer setup for reference. **(b)** Recorded luminescence in the crystallizer volume at 42.2 kHz and a power of 8 W ( $\pm 2$  W); exposure time  $\approx 3$  min.

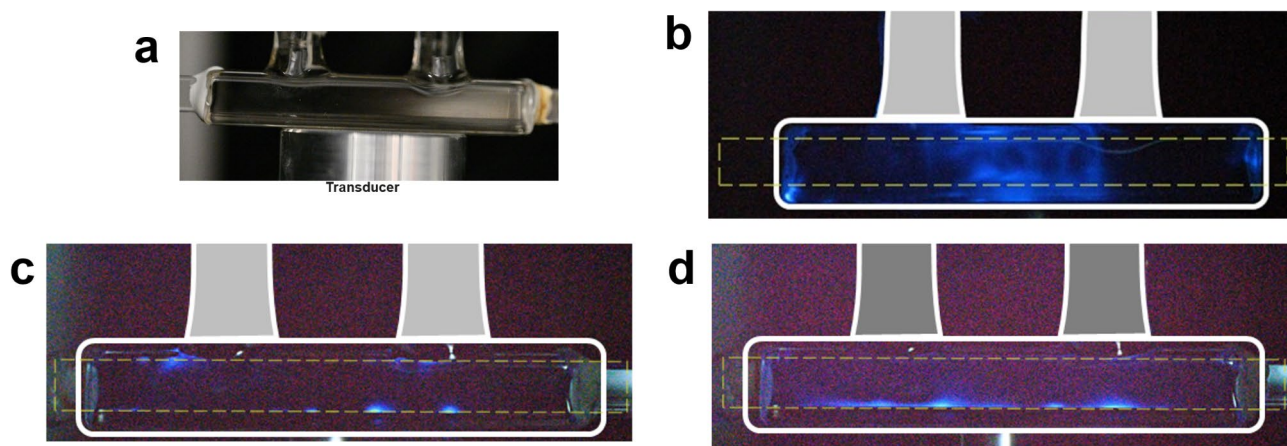


**Fig. 13.** Sonochemiluminescence in flow crystallizer used for ROY single phase experiments. **(a)** Crystallizer setup for reference. **(b)** sonochemiluminescence in the bath of the crystallizer; exposure time  $\approx 25$  s. **(c)** Sonochemiluminescence in the channel of the crystallizer; exposure time  $\approx 3$  min. **(d)** Sonochemiluminescence in the channel of the crystallizer; exposure time  $\approx 5$  min.

in these experiments they were recorded with a high speed camera and the color change in the crystallizer from orange to yellow was tracked over time. Results indicated that the degree of transformation during the crystallization process was significantly enhanced by the application of ultrasound.

In flow crystallization, experiments were conducted at two total flow rates of 2.5 mL/min and 10 mL/min. The results in flow experiments, especially at silent conditions, were contrary to the batch experiments. For instance, at 0.2 VF and 2.5 mL/min the polymorphic outcome in batch experiments was Y whereas in flow experiments this was a mixture of OP and Y. This is hypothesized to be because of the different mixing in the flow crystallizer compared to the batch crystallizer. In the absence of an external mixing source there can be areas of varying supersaturation in the channels which can lead to different polymorphs nucleating. When ultrasound was applied though, the polymorphic form again shifted towards the stable Y form for all VFs. However, at higher flow rates the effect of ultrasound transforming polymorphs to the Y form was weakened. This could be due to the lower residence time which limited the full transformation of the products. CFD modelling of silent

conditions indicated that the crystals first nucleated in areas where the supersaturation was very high. This was a confirmation that in silent flow experiments lack of mixing created supersaturation gradients leading to nucleation of different polymorphic forms.

Overall the results show that ultrasound at low frequencies, where acoustic cavitation manifests itself, can have a significant effect on the polymorphic outcome of compounds like ROY in anti-solvent crystallization systems. This could potentially be because of the enhanced transformation of the metastable forms to the stable form facilitated by ultrasound. This phenomenon, however, occurs when sufficient residence time is provided since it was noticed that the effect diminished with increase in flow rates. This ability of ultrasound could especially be utilized in cases where meta-stable forms need to be eliminated from the product. Moreover, this can also increase the yield of the stable form since the enhancement of transformation was also significant in high supersaturation cases. With the right selection of flow rate/residence time this can also be utilized in a flow crystallization system.

### Data availability

The datasets generated during and/or analysed during the current study are available from the corresponding author on reasonable request.

Received: 20 February 2025; Accepted: 7 April 2025

Published online: 24 April 2025

### References

- Saifee, M., Inamdar, N., Dhamecha, D. L. & Rathi, A. A. Drug polymorphism: A review, (2009). <https://doi.org/10.4314/ijhr.v2i4.55423>
- Llinàs, A. & Goodman, J. M. Polymorph control: past, present and future, (2008). <https://doi.org/10.1016/j.drudis.2007.11.006>
- Ruecroft, G., Hipkiss, D., Ly, T., Maxted, N. & Cains, P. W. Sonocrystallization: the use of ultrasound for improved industrial crystallization. *Org. Process. Res. Dev.* <https://doi.org/10.1021/op050109x> (2005).
- McCausland, L. J., Cains, P. W. & Martin, P. D. Use the power of sonocrystallization for improved properties. *Chem. Eng. Prog.* (2001).
- Nakajima, K. et al. Nucleus factory on cavitation bubble for amyloid B fibril. *Sci. Rep.* **6** (1), 22015. <https://doi.org/10.1038/srep22015> (Feb. 2016).
- Gogate, P. R., Sutkar, V. S. & Pandit, A. B. Sonochemical reactors: important design and scale up considerations with a special emphasis on heterogeneous systems. *Chem. Eng. J.* **166** (3), 1066–1082. <https://doi.org/10.1016/j.cej.2010.11.069> (Feb. 2011).
- Valitov, G., Jamshidi, R., Rossi, D., Gavriilidis, A. & Mazzei, L. Effect of acoustic streaming on continuous flow sonocrystallization in millifluidic channels. *Chem. Eng. J.* **379**, 122221. <https://doi.org/10.1016/j.cej.2019.122221> (Jan. 2020).
- Cogné, C. et al. Theoretical model of ice nucleation induced by acoustic cavitation. Part 1: pressure and temperature profiles around a single bubble. *Ultrason. Sonochem.* <https://doi.org/10.1016/j.ulsonch.2015.05.038> (2016).
- Gracin, S., Uusi-Penttilä, M. & Rasmuson, Å. C. Influence of ultrasound on the nucleation of polymorphs of p-aminobenzoic acid. *Cryst. Growth Des.* <https://doi.org/10.1021/cg050056a> (2005).
- Zhang, D., Xu, S., Du, S., Wang, J. & Gong, J. Progress of pharmaceutical continuous crystallization. *Engineering* <https://doi.org/10.1016/j.eng.2017.03.023> (2017).
- Ziemecka, G., Stroobants, B., Wit & Maes, and Polymorph selection of ROY by Flow-Driven crystallization. *Cryst. (Basel)*. **9**, 351. <https://doi.org/10.3390/cryst9070351> (Jul. 2019).
- Tyler, A. R. et al. Encapsulated nanodroplet crystallization of Organic-Soluble small molecules. *Chem* **6** (7), 1755–1765. <https://doi.org/10.1016/j.chempr.2020.04.009> (Jul. 2020).
- Van Nerom, M. et al. The effect of controlled mixing on ROY polymorphism. *Cryst. (Basel)*. **12** (5). <https://doi.org/10.3390/cryst12050577> (May 2022).
- Sadegh Cheri, M., Latifi, H., Salehi Moghaddam, M. & Shahraki, H. Simulation and experimental investigation of planar micromixers with short-mixing-length. *Chem. Eng. J.* **234**, 247–255. <https://doi.org/10.1016/j.cej.2013.08.067> (Dec. 2013).
- Coliaie, P., Kelkar, M. S., Nere, N. K. & Singh, M. R. Continuous-flow, well-mixed, microfluidic crystallization device for screening of polymorphs, morphology, and crystallization kinetics at controlled supersaturation. *Lab. Chip.* **19**, 2373–2382. <https://doi.org/10.1039/C9LC00343F> (2019).
- Chen, X. & Shen, J. Numerical and experimental investigation on splitting-and-recombination micromixer with E-shape mixing units. *Microsyst. Technol.* **23** (10), 4671–4677. <https://doi.org/10.1007/s00542-016-3208-5> (Oct. 2017).
- Nogueira, B. A., Castiglioni, C. & Fausto, R. Color polymorphism in organic crystals. *Commun. Chem.* **3** (1), 34. <https://doi.org/10.1038/s42004-020-0279-0> (Mar. 2020).
- Threlfall, T. Structural and Thermodynamic Explanations of Ostwald's Rule, *Org Process Res Dev*, vol. 7, no. 6, pp. 1017–1027, Nov. (2003). <https://doi.org/10.1021/op030026l>
- Skorb, E. V., Möhwald, H. & Andreeva, D. V. Effect of cavitation bubble collapse on the modification of solids: crystallization aspects. *Langmuir* **32**, 11072–11085. <https://doi.org/10.1021/acs.langmuir.6b02842> (Nov. 2016).
- Tanaka, K. & Takiyama, H. Effect of Oiling-Out during crystallization on purification of an intermediate compound. *Org. Process. Res. Dev.* **23** (9), 2001–2008. <https://doi.org/10.1021/acs.oprd.9b00256> (Sep. 2019).
- Lee, J. & Yang, S. Antisolvent sonocrystallisation of sodium chloride and the evaluation of the ultrasound energy using modified classical nucleation theory. *Cryst. (Basel)*. <https://doi.org/10.3390/cryst8080320> (2018).
- Kubota, N. Analysis of the effect of volume on induction time and metastable zone width using a stochastic model. *J. Cryst. Growth*. **418**, 15–24. <https://doi.org/10.1016/j.jcrysgro.2015.02.021> (May 2015).
- Rossi, D. et al. Continuous-Flow sonocrystallization in Droplet-Based microfluidics. *Cryst. Growth Des.* <https://doi.org/10.1021/acs.cgd.5b01153> (2015).

### Acknowledgements

The research leading to these results has received funding from VLAIO (Catalisti) in the MMICAS project HBC.2020.2627.

### Author contributions

M.N.H: Conceptualization, methodology, investigation, data processing, writing- original draft. A.D: Investigation, data processing, writing. T.V.G: Conceptualization, methodology, resources, review & editing, supervision,

funding acquisition.

## Declarations

### Competing interests

The authors declare no competing interests.

### Additional information

**Supplementary Information** The online version contains supplementary material available at <https://doi.org/10.1038/s41598-025-97635-7>.

**Correspondence** and requests for materials should be addressed to M.N.H.

**Reprints and permissions information** is available at [www.nature.com/reprints](http://www.nature.com/reprints).

**Publisher's note** Springer Nature remains neutral with regard to jurisdictional claims in published maps and institutional affiliations.

**Open Access** This article is licensed under a Creative Commons Attribution-NonCommercial-NoDerivatives 4.0 International License, which permits any non-commercial use, sharing, distribution and reproduction in any medium or format, as long as you give appropriate credit to the original author(s) and the source, provide a link to the Creative Commons licence, and indicate if you modified the licensed material. You do not have permission under this licence to share adapted material derived from this article or parts of it. The images or other third party material in this article are included in the article's Creative Commons licence, unless indicated otherwise in a credit line to the material. If material is not included in the article's Creative Commons licence and your intended use is not permitted by statutory regulation or exceeds the permitted use, you will need to obtain permission directly from the copyright holder. To view a copy of this licence, visit <http://creativecommons.org/licenses/by-nc-nd/4.0/>.

© The Author(s) 2025